Communication

New Insights into Ethene Epoxidation on Two Oxidized Ag{111} Surfaces

Marie-Laure Bocquet, Angelos Michaelides, David Loffreda, Philippe Sautet, Ali Alavi, and David A. King

J. Am. Chem. Soc., **2003**, 125 (19), 5620-5621• DOI: 10.1021/ja0297741 • Publication Date (Web): 17 April 2003

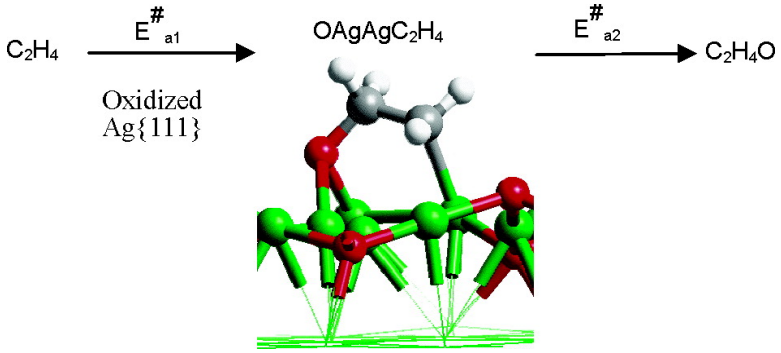

More About This Article

Additional resources and features associated with this article are available within the HTML version:

- Supporting Information
- Links to the 11 articles that cite this article, as of the time of this article download
- Access to high resolution figures
- Links to articles and content related to this article
- Copyright permission to reproduce figures and/or text from this article

View the Full Text HTML

J|A|C|S
COMMUNICATIONS

Published on Web 04/17/2003

New Insights into Ethene Epoxidation on Two Oxidized Ag{111} Surfaces

Marie-Laure Bocquet,*,† Angelos Michaelides,‡ David Loffreda,† Philippe Sautet,† Ali Alavi,‡ and David A. King‡

Laboratoire de Chimie, UMR 5532, Ecole Normale Supérieure, Lyon, France, and Department of Chemistry, University of Cambridge, Lensfield Road, Cambridge, CB2 1EW, U.K.

Received December 17, 2002; E-mail: mbocquet@ens-lyon.fr

Ethene epoxidation is an important heterogeneous catalysis process that takes place selectively on silver catalysts. The mechanism of this partial oxidation has been debated for many years, and to date a detailed atomic level understanding of this process has not been obtained. Much of the debate has centered on the nature of the active O species.[1,2] Recently, two stable O phases on Ag{111} have been characterized with the scanning tunneling microscope (STM) and density functional theory (DFT).[3,4] One is a low coverage (0.05 ± 0.02 ML) O adatom phase, and the other is an $Ag_{1.8}O$ oxide overlayer. A DFT-derived phase diagram predicted that the $Ag_{1.8}O$ oxide overlayer would be stable under typical industrial conditions for epoxidation.[4] However, the temperature and pressure boundaries with the low coverage O adatom phase were close, implying that both phases could easily coexist in a reactor. Additionally, Barteau and co-workers made a significant step forward with the identification and characterization of a surface oxametallacycle on Ag{111} (labeled OME or OMME if they include one or more than one surface atoms, respectively).[5] With the aid of high-resolution electron energy loss spectroscopy (HREELS) and DFT-based cluster calculations, they showed that this was a precursor to ethene epoxide formation.[6] However, that study focused on a single elementary step for the reverse reaction starting with epoxide.

The partial oxidation reaction, $C_2H_4 + {}^1/_2O_2 \rightarrow C_2H_4O$, is exothermic by 117 kJ/mol at room temperature, and so the conversion is merely inhibited by kinetics. In this work, we use periodic DFT to determine accurate values for the kinetic barriers to the formation of ethene epoxide. Reaction mechanisms and their associated barriers for the complete catalytic cycle of the conversion of ethene to epoxide have been determined on the recently characterized low and high coverage oxygen phases. We find that on both catalysts epoxidation proceeds similarly via a two-step nonconcerted process. Concerted mechanisms in which O adds across the C═C bond, directly producing epoxide, have been ruled out. The key implications are that both surfaces are active and that epoxidation can take place over a wide O coverage regime.

Calculations were performed within the plane-wave pseudopotential formalism of DFT. Two codes, VASP[7] and CASTEP,[8] were used to investigate epoxidation at high and low O coverages, respectively. These codes utilize ultrasoft pseudopotentials and the Perdew Wang (PW91) generalized gradient approximation.[9] It has been shown that good structural and energetic agreement between these two codes can be achieved.[4] Three-layer Ag slabs in p(4 × 4) unit cells, with a vacuum region equivalent to six Ag layers, were used throughout. The low coverage O phase was modeled by placing a single O, corresponding to a coverage of 0.0625 ML, in the p(4 × 4) cell and will be noted Ag{111} + O. The high coverage oxide phase consisted of an $Ag_{1.8}O$ oxide trilayer adsorbed on top of the three-layer Ag{111} slab. All energies are obtained with **k**-point sampling equivalent to 64 symmetric points in the Brillouin zone of a (1 × 1) cell. However, because of the increased complexity of calculations involving the oxide overlayer for these systems, this **k**-point sampling was used to obtain energies based on structure optimizations performed with **k**-point sampling equivalent to 16 symmetric points. Transition states were identified with constrained minimization techniques and verified by the presence of a single imaginary mode from an additional vibrational frequency analysis.[10]

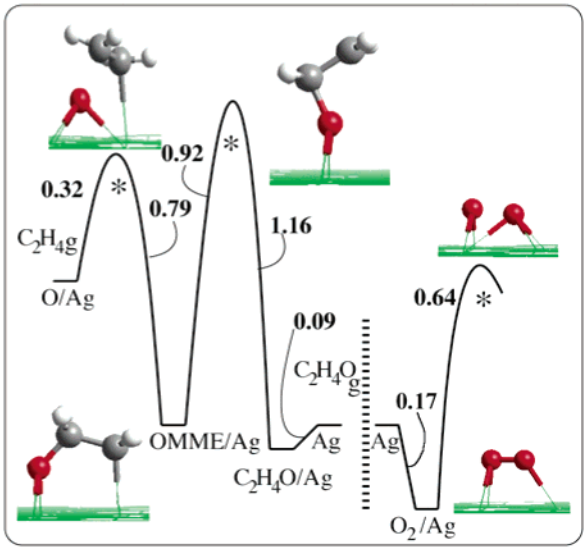

Figure 1. Relative energy diagram for the conversion of gas-phase ethene into ethene epoxide (C_2H_4O) via an oxametallacycle (OMME) intermediate on Ag{111} + O. Energies shown in eV refer to the differences between adjacent equilibrium states, or between adjacent equilibrium and transition states. States to the right-hand side of the vertical dashed line do not contain epoxide molecules and are simply related to O_2 dissociative adsorption on clean Ag{111} (O, red; C, gray; *, transition state).

The energy profile determined for the oxidation of ethene to ethene epoxide at low O coverage on Ag{111} is shown in Figure 1. We find that epoxidation occurs through a two-step process via an OMME intermediate. The barrier for the first step, which proceeds through an Eley−Rideal type mechanism, is 0.32 eV. This produces a chemisorbed OMME which is 0.47 eV more stable than the initial state of chemisorbed O and gas-phase ethene. In this OMME intermediate, O is at a bridge site, and the O−C−C backbone linkage sits across a three-fold site with one of the carbons bonding directly to the surface. This OMME is the most stable of eight oxametallacycles investigated, and its structure is similar[11] to that predicted by previous cluster calculations.[6,12] A barrier of 0.92 eV was then identified for OMME ring closure to produce a weakly adsorbed ethene epoxide (0.09 eV). To determine the

† Ecole Normale Supérieure.
‡ University of Cambridge.

10.1021/ja0297741 CCC: $25.00

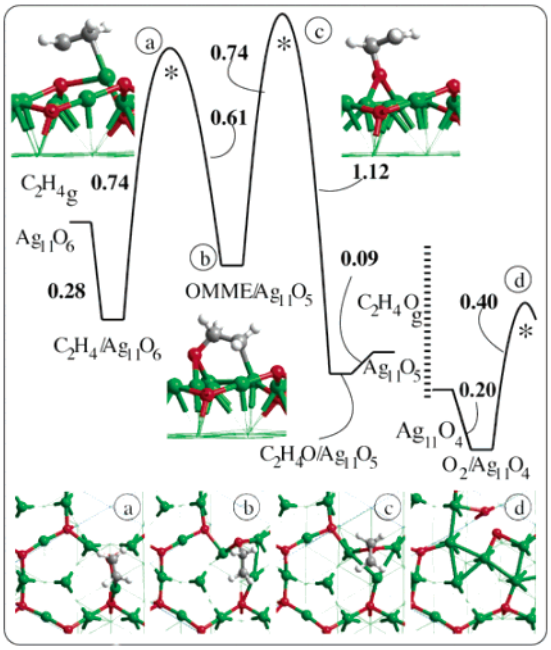

Figure 2. Relative energy diagram similar to Figure 1 for the conversion of gas-phase C_2H_4 to epoxide, except here on the high coverage $Ag_{1.8}O$ ($Ag_{11}O_6$) layer on Ag{111}. On the right side of the vertical dashed line, O_2 dissociative adsorption on an O-deficient $Ag_{11}O_4$ oxide is displayed. The panels (a)−(d) correspond to the top views of the intermediate states labeled (a)−(d) (O, red; C, gray; Ag, green; *, transition state).

energetics of the entire catalytic cycle, the dissociation of O_2 on clean Ag{111} was also examined as the last regeneration step. A barrier of 0.64 eV, relative to a weakly adorbed O_2 precursor state (E_{ads} = 0.17 eV), has been determined for this process.

The energetic profile for epoxidation on the high coverage $Ag_{1.8}O$ oxide surface is displayed in Figure 2. A weak ethene adsorption precursor is first seen. This state (not shown) has recently been characterized in a combined STM and DFT study[13] and shows ethene symmetrically adsorbed above an Ag of the oxide ring. The barrier to produce the OMME from this state is 0.74 eV (0.46 eV relative to the initial C_2H_4 gas-phase state). At the transition state, a C−O bond has been created through a lateral shift of ethene toward an adjacent oxygen in the underlying oxide. The structure of the OMME product of this step is 0.15 eV more stable than the initial state (with C_2H_4 in the gas phase). It is worth noting that the extraction of an O from the oxide has resulted in a significant reconstruction of the oxide ring. In the next step, the second C−O bond is formed to produce an epoxide with a barrier of 0.74 eV. The epoxide binds weakly to the oxygen-deficient oxide (0.09 eV), above a triangle of Ag atoms. To mimic an entire catalytic cycle, a second O was removed from the oxide overlayer (equivalent to performing a second epoxidation cycle), and O_2 dissociation was examined on this doubly reduced oxide overlayer. The most favorable dissociation route identified, with a barrier of 0.40 eV, through the transition state labeled (d) in Figure 2, involves O_2 initially adsorbed parallel to the surface.

Overall, we see that on the two surfaces examined the epoxidation mechanisms are reasonably similar, in terms of both structures and energies. On both catalysts, epoxidation proceeds via an OMME intermediate, and it is the ring closure of this OMME intermediate that is the most highly activated step of the cycle (with a barrier of 0.74 eV on the oxide and 0.92 eV on the O adatom phase). This lower barrier to OMME ring closure on the oxide surface could be explained by the reduced stability of the OMME intermediate on this surface. If we compare the barriers determined here to those from experiment, we find that satisfyingly they fall within the broad range reported (0.6−1.1 eV[14,15]). Other differences between the two substrates arise in the OMME formation step (first step) and the catalyst regeneration step (O_2 dissociation). Ethene is first trapped into a chemisorption state before reacting on the oxide, whereas on the O adatom phase it reacts directly from the gas phase. However, we anticipate that this state, with moderate binding of ethene to the oxide, will not be populated at reaction temperatures. This would render the first step similar on both surfaces. Finally, O_2 dissociation is favored on the reduced oxide surface ($Ag_{11}O_4$ in Figure 2), with a barrier of 0.40 eV as opposed to 0.64 eV on clean Ag{111}. Given that the reduced $Ag_{11}O_4$ oxide surface is unstable as compared to the equilibrium $Ag_{1.8}O$ ($Ag_{11}O_6$) oxide overlayer, a low barrier to O_2 dissociation on this surface is to be anticipated.

In conclusion, mechanisms and barriers for the conversion of ethene to ethene epoxide on two oxidized Ag surfaces have been determined. On both catalysts, epoxidation proceeds via an oxametallacycle intermediate, and it is the ring closure of this intermediate that is the most highly activated step. The particular question of which catalyst is a priori the most reactive goes beyond the present study and will be the subject of future kinetic modeling. Here, we conclude that both oxidized surfaces are efficacious selective oxidation catalysts and that Ag may act as a dual phase catalyst inside the reactor.

Acknowledgment. A.M. wishes to thank Gonville and Caius College, Cambridge, for a research fellowship. M.-L.B., D.L., and P.S. thank IDRIS for CPU time through Project 609.

Supporting Information Available: Geometries of the most important intermediates and transition states (PDF). This material is available free of charge via the Internet at http://pubs.acs.org.

References

(1) van Santen R. A.; Kuipers, H. P. C. *Adv. Catal.* **1987**, *35*, 265 and references therein.
(2) Campbell, C. T. *J. Catal.* **1985**, *94*, 436.
(3) Carlisle, C. I.; King, D. A.; Bocquet, M.-L.; Cerda, J.; Sautet, P. *Phys. Rev. Lett.* **2000**, *84*, 3899.
(4) Michaelides, A.; Bocquet, M.-L.; Sautet, P.; Alavi, A.; King, D. A. *Chem. Phys. Lett.* **2003**, *367*, 344.
(5) Jones, G. S.; Mavrikakis, M.; Barteau, M. A.; Vohs, J. M. *J. Am. Chem. Soc.* **1998**, *120*, 3196.
(6) Linic, S.; Barteau, M. A. *J. Am. Chem. Soc.* **2002**, *124*, 310.
(7) Kresse, G.; Furthmüller, J. *Comput. Mater. Sci.* **1996**, *6*, 15; *Phys. Rev. B* **1996**, *54*, 11169.
(8) CASTEP 4.2 Academic Version, licensed under the UKCP-MSI Agreement, 1999; Payne, M. C., et al. *Rev. Mod. Phys.* **1992**, *64*, 1045.
(9) Perdew, J. P.; Chevary, J. A.; Vosko, S. H.; Jackson, K. A.; Pederson, M. R.; Singh, D. J.; Fiolhais, C. *Phys. Rev. B* **1992**, *46*, 6671.
(10) Michaelides, A.; Hu, P. *J. Am. Chem. Soc.* **2001**, *123*, 4235.
(11) Some discrepancy is found with the relative stability of the OMME and epoxide states as compared to the DFT results of ref 6. Possibly this is due to the different surface models used here and in ref 6.
(12) Saravanan, C.; Salazar, M. R.; Kress, J. D.; Redondo, A. *J. Phys. Chem. B* **2000**, *104*, 8685.
(13) Bocquet, M.-L.; Sautet, P.; Cerda, J.; Carlisle, C. I.; Webb, M.; King, D. A. *J. Am. Chem. Soc.* **2003**, *125*, 3119.
(14) Campbell, C. T. *Surf. Sci.* **1984**, *139*, 396.
(15) Berty, J. M. *Applied Industrial Catalysis*; Academic Press: New York, 1983; Vol. 1, Chapter 8.

JA0297741